MALAYSIAN JOURNAL OF COMPUTING AND APPLIED MATHEMATICS (2020) 3 (2) 1-24

DOI: *https://doi.org/10.37231/myjcam.2020.3.2.46*

Article: Received 31.08.2020; Accepted 21.10.2020; Published 04.12.2020

COMPARISON OF PICARD AND NEWTON ITERATIVE SCHEMES IN THE FINITE ELEMENT MODELING FOR ONE-DIMENSIONAL VARIABLY SATURATED-UNSATURATED FLOWS

M S Islam[a,✉], R Ahamad[b]

[a,b]Department of Mathematics, Shahjalal University of Science & Technology, Sylhet-3114, Bangladesh.
✉sislam_25@yahoo.com

Abstract: Numerical simulation of saturated-unsaturated flow in porous media is of incredible enthusiasm for some parts of science and engineering, for example, agricultural engineering, ground water the managements, petroleum reservoir, bioenvironmental processes, chemical contaminants tracing, and so on. Demonstrating of fluid flow in variably saturated-unsaturated porous media generally brings about systems of highly nonlinear partial differential equations, Richards' equation, which are not reasonable diagnostically except if ridiculous and distorting presumptions are made with respect to the attributes, flow dynamics, and properties of the physical frameworks. Because of the pertinence of the physical frameworks it portrays and the challenges related with its solution, significant exertion has been given to generating exact, strong, and efficient numerical strategies for Richards' equation. Among the different numerical simulation techniques accessible, the finite element strategy is worthwhile in light of the fact that it offers simplicity of discretization with low order time integration approaches to explain Richards' equation. Picard and Newton methods are the most usually practiced iterative methods for the numerical solution of the nonlinear coupled systems. A finite element numerical model was developed to precisely and efficiently figure a solution of the nonlinear Richards' equation with homogeneous and layered soil. In this work, we have considered these two regular iterative strategies which can be utilized in a solution methodology for the nonlinear Richards' equation governing flow in variably saturated-unsaturated porous media. We have evaluated the efficiency, accuracy, robustness and computational efficacy of the iterative Newton and Picard methods. The assessments depend on three distinctive test issues of one-dimensional saturated-unsaturated flow with homogeneous and heterogeneous soil properties. Besides, spatial adjustment will be founded on a fine spatial discretization and temporal adjustment will be practiced employing variable order, variable step size dependent on the backward Euler finite difference formula. The computed results obviously demonstrated that the methodology was computationally productive, yet additionally increasingly precise and robust. Computational execution was significantly improved with the Picard strategy, and which could be applied to simulate heterogeneous soil and Newton scheme is superior for homogeneous soil materials.

Keywords: *Richards' equation; Numerical solution; Finite element; Picard and Newton methods; Variably saturated-unsaturated flows*.

1. INTRODUCTION

The forecast of fluid motion in unsaturated soil is a significant issue in numerous parts of science and engineering. In all research studies of the unsaturated zone, fluid movement is accepted to comply with the classical nonlinear Richards' equation. The nonlinear Richards' equation in variably permeable media should be tackled numerically with constitutive relations, heterogeneities, unpredictable geometries, and complex boundary conditions. The solution of this equation, both analytical and numerical, is very challenging because of the strong nonlinear relationships that association soil moisture to soil hydraulic conductivity and pressure-head. For instance, when the constitutive connection is extremely nonlinear and the present status is totally different from the solution state, the size of the time step ought to be restricted for simulations of dynamically saturated flow, to cause the iterative systems to converge and to safeguard small changes in saturation or the pressure head in any piece of the region during the time step. Such

characteristic troubles in solving the Richards' equation have seriously restricted its different applications, including coupled surface and subsurface water development issues, which at the same time simulate subsurface water flow in the unsaturated and saturated zones, just as mind boggling territorial scale issues depicting groundwater flow.

Modeling of fluid flow in dynamically saturated-unsaturated porous media as a rule brings about frameworks of exceptionally nonlinear parabolic partial differential equations which are not solvable analytically except if unreasonable and distorting presumptions are made in regards to the characteristics, dynamics, and properties of the physical frameworks [1-3]. Such mathematical relation is described by the Richards' equation, which was formulated by applying unsaturated Darcy's law and continuity equation [4]. Therefore, the Richards' equation is generally applicable and can be used for fundamental research and scenario analysis for variably saturated-unsaturated flow.

Numerical solution of Richards' equation by current schemes generally decouples the issues of temporal and spatial discretization and resolution methods. These choices influence computational time, numerical stability and result accuracy. Numerical strategies for Richards' equation have pulled in extensive exploration consideration and are broadly utilized in commonsense recreations of subsurface procedures. But many studies have been shown that general numerical techniques can't take care of certain flow issues adequately, especially for those that give rise to sharp wetting fronts, drainage, perched water tables, flow through heterogeneous materials, infiltration into initially dry soils with non-uniform pore size distribution [5]. This examination explores the upsides of noniterative versatile time stepping strategies for Richards' equation and built up a straightforward practical approximation that takes care of these troublesome issues precisely. The proposed model is firmly identified within backward Euler algorithms and thus can be utilized to improve existing programming for useful subsurface simulations. There are a number of commercial software tools available that have been specifically designed for the solution of the three-dimensional Richards' equation for porous flow problems; for example, the codes SWMS-3D [6], 3DFEMFAT [7], SVFLUX [8] and FEMWATER [9]. However, there are now a series of general-purpose commercial computational fluid dynamics (CFD) codes available [10, 11, 12], which enable a vast array of complex thermo-fluid physics to be represented.

Because of the pertinence of the physical frameworks it portrays and the challenges related with its answer, noteworthy exertion has been given to developing exact, vigorous, and proficient numerical techniques for Richards' equation. The standard methodologies utilized finite difference or finite element spatial approximations with low order time integration methods to tackle Richards' equation, which are normally communicated in three standard structures: pressure head based, moisture content based and mixed structure where the two variables are utilized. The head-based model can be embraced to manage both saturation and unsaturation conditions. Notwithstanding, for exceptionally non-linear issues, for example, infiltration into dry soils, these strategies may experience the ill effects of mass-balance error, convergence issues and helpless iterative effectiveness [12, 13]. Work has continued in numerous territories, including time integration approaches combined with finite difference or finite element spatial approximations [14]. The time stepping approximations included backward Euler and related algorithms [e.g., 15, 16]. A fundamental research in the numerical examination of Richards' equation is the presentation of adaptive time stepping calculations, which conform to the conduct of the solution and are commonly consistent and more efficient than uncontrolled schemes. Adaptation of spatial approximations for Richards' equation includes a hierarchic finite element algorithm [17] and a front-tracking algorithm [18]. The use of a few existing variable-order variable-step size differential algebraic equation solvers (DASPK) [12, 19, 20] and lower-order adaptive backward Euler and related schemes [13, 15] are described and applied to the pressure head-based Richards' equation. Modern high-order techniques gave considerable enhancements over existing low-order uniform step size schemes when a very small nonlinear tolerance is specified. In any case, numerous ordinary differential equation schemes have certain restrictions in the pragmatic setting of modeling variably saturated flows. In all cases, formal truncation error control prompts significant increases in exactness and effectiveness over fixed step and heuristic time stepping calculations and furthermore progresses the mass balance of procedures dependent on pressure head type of Richards' equation.

Method of lines approach has been utilized to present adaptive, higher order time discretizations with formal error control for settling Richards' equation. The characteristics of a technique for method of lines approach along with a differential algebraic equation solver have been analyzed for a scope of Richards'

equation issues utilizing standard finite difference spatial discretizations [19]. This methodology has shown various focal points regarding efficiency and accuracy and speaks to a promising reason for building vigorous solvers fit for simulating troublesome dynamically saturated flow issues [12, 21]. Mixed finite element techniques have gotten huge consideration in the water resources field as of late on the grounds that they produce exact, mass-preservationist velocity fields with constant typical segments and are pertinent for frameworks with heterogeneous material properties and unpredictable geometries [22]. Mixed finite element techniques have discretizations have been applied to a scope of groundwater flow problems [22]. In particular, a few mixed finite element techniques have approaches have been utilized to model Richards' equation employing standard low-order time discretizations with either fixed time step or exactly based adaption [23]. The upsides of the method of lines over low-order approximations for Richards' equation by applying finite difference spatial discretizations propose that there may be comparable advantages for a mixed finite element strategies discretization inside a method of lines setting. This might offer a powerful methodology that is precise in both time and space for a scope of sensible conditions including sporadic, heterogeneous areas. A standard finite element strategies discretization, notwithstanding, can prompt linear system that are ineffectively molded and especially hard to comprehend for enormous time steps or steady-state conditions [23]. Various varieties of the mixed finite element strategy have been created to address this deficiency. For instance, the mixed-hybrid finite element procedure acquaints Lagrange multipliers with decrease the original finite element strategies issue to one with a superior molded linear system [22]. Then again, the utilization of a mixed-hybrid finite element technique discretization needs some clear change of the standard technique for a method of lines tactic [24]. Furthermore, the fixed time integrators not have prevalence and are computationally wasteful. Unconditional stability is a significant possession of an efficient time stepping scheme for Richards' equation, due to the stiffness of spatially discrete parabolic partial differential equations [13, 14]. In fact, most invent and research codes employ the first order accurate and stable implicit Euler algorithm.

Picard and Newton methods are the most frequently utilized iterative techniques for the numerical solution of the nonlinearity coupled frameworks [15, 25]. Several authors [25, 26, 27] have demonstrated that the Newton scheme may be more competent in some specific flow cases than the Picard scheme. Newton-type techniques have additionally been applied, including the initial-slope Newton scheme, Newton-Krylov methods, and combined Picard-Newton schemes [23, 28, 29]. Eventually, Picard emphasis is the most well-known because of its straightforwardness and for the most part adequate presentation [27]. Be that as it may, Picard and Newton solvers in uncontrolled time stepping processes produce deficient convergence conduct or complete disappointment for certain unconsolidated looms and clay looms. Progressively complex variable-order variable-step techniques with chord slope solvers, just as Newton solvers upgraded with global line searches can be utilized to enhance convergence rate in these troublesome simulations [5, 19]. Iterative solvers are computationally costly on account of different emphases are remembered for the recalculation for Jacobian matrix at each time step.

The main purpose of this research is to generalize the pressure head-based finite element algorithm to handle the nonlinearity, minimize the mass balance errors locally and globally of the flow equation and applications of one-dimensional saturated-unsaturated flow conditions. This is accomplished by linearizing a head-based flow equation with the Picard and Newton iteration methods. A conventional Galerkin finite element method is then used to solve the linearized formulation to obtain the solution of flow problems. Other principle goals are to numerically decide the request for precision and to analyze the computational proficiency of the two methods, just as to research the distinctions in execution between these two iterative procedures. Computational efficiency will be measured on the basis of CPU time expended to achieve a given level of accuracy. To evaluate the efficiency and robustness, numerical experiments will be presented to illustrate the promising solution performance of the iteration methods which will be made by fine grid maintain with a tight nonlinear tolerance for the test problems.

2. NUMERICAL PROCEDURES

Governing Equations

Three standard forms of Richards' equation are identified by the mixed ('$\psi - \theta'$), the pressure head ('ψ')-based and the water content ('θ')-based forms. Both the pressure head and the water content are the primary solved variable. The constitutive relationship between fluid/moisture content and pressure head allows for conversion of one form of the equation to another. For one-dimensional vertical flow, the 'ψ-based' form, where the primary variable is the pressure head, can be written as follows:

$$\mathrm{C}(\psi)\frac{\partial \psi}{\partial \mathrm{t}} = \frac{\partial}{\partial \mathrm{z}}\left(\mathrm{K}(\psi)\left(\frac{\partial \psi}{\partial \mathrm{z}} + 1\right)\right) \tag{1}$$

where, $C(\psi)$ is the specific fluid capacity [L^{-1}] and is defined by $C(\psi) = \frac{d\theta}{d\psi}$, ψ is the pressure head [L], t is time [T], z denotes the vertical distance from reference elevation, assumed positive upward [L], $K(\psi)$ is the hydraulic conductivity [LT^{-1}], and θ is the moisture content.

It is convoluted to offer any explicit expressions about the appropriateness of every one of the various structures, a few patterns have been watched. With the pressure head structure of Richards' equation, the governing mathematical model is planned as far as pressure head before the real discretization. This formulation is more flexible and appropriate to both saturated and unsaturated phenomena but numerical simulation is much expensive due to its strong nonlinearity in the soil hydraulic relations. In any case, this model likewise delivers poor global mass balance for dry initial conditions just as for issues including infiltration into extremely dry soils. The reason for poor mass balance resides in the time derivative term. While $\frac{d\theta}{dt}$ and $C(\psi)\left(\frac{d\psi}{dt}\right)$ are mathematically equivalent in the continuous partial differential equation, their discrete analogues are not. The inequality in the discrete forms is exacerbated by the high nonlinearity of the specific capacity term $C(\psi)$. This prompts noteworthy mass-balance errors in the ψ-based formulations because the change in mass in the system is calculated using discrete values of $\frac{d\theta}{dt}$ while the approximating equations use the expansion $C(\psi)\left(\frac{d\psi}{dt}\right)$. Exceptionally fine spatial and temporal discretizations mass lumping are expected to keep up mass balance property for these circumstances. Employing regular time-integration techniques, mass-balance errors increase with the time-step size. Moreover, mass preservation isn't consequently ensured despite the fact that the subsequent error can be limited by appropriate assessment of the capacitance [30]. Various approaches have been developed to overcome such difficulties. A mass-conserving solution that modifies the capacity term to force global mass balance scheme is proposed [31]. A mass distributed algorithm that satisfied mass balance and was free from oscillation [32]. Implementation of method of lines is shown the property of good mass balance through time-step truncation error [19].

Equations for Soil Hydraulic Properties

Richards' equation must be completed with the connection between the pressure head, water content, and hydraulic conductivity, describing the soil hydraulic properties. There are several mathematical relationships for the constitutive or soil water retention curves that are used in modeling. Next two of the most frequently applied models, to be specific the Brooks-Corey [33] model and van Genuchten model [34]. These two models are described as follows:

Brooks–Corey Model

The constitutive relationships proposed by Brooks and Corey [33] are given by:

$$\theta(\psi) = \theta_r + (\theta_s - \theta_r)\left(\frac{\psi_d}{\psi}\right)^n \text{ if } \psi \leq \psi_d \tag{2}$$

$$\theta(\psi) = \theta_s \, if \, \psi > \psi_d \tag{3}$$

$$K(\psi) = K_s\left[\frac{\theta(\psi) - \theta_r}{\theta_s - \theta_r}\right]^{3+2/n} \text{ if } \psi \leq \psi_d \tag{4}$$

$$K(\psi) = K_s \text{ if } \psi > \psi_d \tag{5}$$

$$C(\psi) = n\frac{\theta_s - \theta_r}{|\psi_d|}\left(\frac{\psi_d}{\psi}\right)^{n+1} \text{ if } \psi \leq \psi_d \tag{6}$$

$$C(\psi) = 0 \text{ if } \psi > \psi_d \tag{7}$$

where θ_s is the saturated moisture content [L^3L^{-3}], θ_r is the residual moisture content [L^3L^{-3}], $\psi_d = -\frac{1}{\alpha}$ is the bubbling or air entry pressure head [L] and is equal to the pressure head to desaturate the largest pores in the medium and $m = 1 - \frac{1}{n}$ is a pore-size distribution index (dimensionless).

van Genuchten Model

Perhaps the most widely-used constitutive relations for moisture content and hydraulic conductivity are those of van Genuchten [34]. The model is given by:

$$\theta(\psi) = \theta_r + \frac{\theta_s - \theta_r}{[1 + |\alpha\psi|^n]^m} \text{ if } \psi \leq 0 \tag{8}$$

$$\theta(\psi) = \theta_s \text{ if } \psi > 0 \tag{9}$$

$$K(\psi) = K_s\left[\frac{\theta - \theta_r}{\theta_s - \theta_r}\right]^{0.5}\left\{1 - \left[1 - \left(\frac{\theta - \theta_r}{\theta_s - \theta_r}\right)^{\frac{1}{m}}\right]^m\right\}^2 \text{ if } \psi \leq 0 \tag{10}$$

$$K(\psi) = K_s \text{ if } \psi > 0 \tag{11}$$

$$C(\psi) = \alpha mn\frac{\theta_s - \theta_r}{[1 + |\alpha\psi|^n]^{m+1}}|\alpha\psi|^{n-1} \text{ if } \psi \leq 0 \tag{12}$$

$$C(\psi) = 0 \text{ if } \psi > 0 \tag{13}$$

Spatial Approximation

The benchmark Galerkin's finite element technique suggests an advantageous method to split the boundary value spatial component of Richards' equation from its initial-value temporal variety and this methodology is especially basic and widely exploit in practice. To build up the finite element guess of the pressure head-based Richards' equation, weak formulation of the dependent variable and the characteristic relations were approximated applying interpolating polynomials [35, 36]. It was accepted that the water driven conductivity just as capacitance changes linearly inside every component [37].

For the numerical solution of Richards' equation (1), we discretize the spatial region employing the finite element Galerkin conspire and the time derivative term utilizing a finite difference strategy. To build up the finite element model, there are $M - 1$ discretized components for M global nodes in the problem space.

So, let us consider the approximating function

$$\psi(z,t) \approx \hat{\psi}(z,t) = \sum_{J=1}^{M} N_J(z)\psi_J(t) \tag{14}$$

where $N_J(z)$ and $\psi_J(t)$ are linear Lagrange basis functions and nodal values of ψ at time t, respectively. Weighted residual procedure is used to solve the unknown coefficients. In local coordinate space $-1 \leq \xi \leq 1$, the approximating function for each element (e) is $\hat{\psi}^{(e)} = \sum_{i=1}^{2} N_i^{(e)}(\xi)\,\psi_i^{(e)}(t) = \frac{1}{2}(1 - \xi)\psi_1^{(e)}(t) + \frac{1}{2}(1 + \xi)\psi_2^{(e)}(t)$, which we can write in vector form as $\hat{\psi}^{(e)} = \left(\boldsymbol{N}^{(e)}(\xi)\right)^T \boldsymbol{\Psi}^{(e)}(t)$. Using the above relations, the equation (14) becomes:

$$\hat{\psi} = \sum_{e=1}^{M-1}(\boldsymbol{N}^{(e)})^T\boldsymbol{\Psi}^{(e)} = \sum_{e=1}^{M-1}\hat{\psi}^{(e)} \tag{15}$$

The following system of ordinary differential equations will obtain by applying the symmetric weak formulation of Galerkin's method the pressure-head form of Richards' equation:

$$\boldsymbol{A}(\boldsymbol{\Psi})\boldsymbol{\Psi} + \mathbf{F}(\boldsymbol{\Psi})\frac{\mathrm{d}\boldsymbol{\Psi}}{\mathrm{dt}} = \mathbf{q}(\mathrm{t}) - \mathbf{b}(\boldsymbol{\Psi}) \tag{16}$$

where $\boldsymbol{\Psi}$ is the pressure head values at the spatial nodes, **A** is the stiffness or conductivity matrix, **F** is the storage or mass matrix, it is noted that stiffness and mass matrices are the function of $\boldsymbol{\Psi}$, **q** contains the specified Darcy flux boundary conditions and **b** contains the gravity drainage term. The dimensionality of the problem and the method of approximation techniques are the causes of the formation of **A**, **F** and **b**. In this study, over local subdomain element $\boldsymbol{\Omega}^{(e)}$, we evaluate these components along the following relations:

$$\boldsymbol{A}^{(e)} = \int_{\boldsymbol{\Omega}^{(e)}} \boldsymbol{K}_s^{(e)} K_r(\hat{\psi}^{(e)}) \frac{\boldsymbol{dN}^{(e)}}{\boldsymbol{dz}} (\frac{\boldsymbol{dN}^{(e)}}{\boldsymbol{dz}})^T dz \tag{17}$$

$$\boldsymbol{b}^{(e)} = \int_{\boldsymbol{\Omega}^{(e)}} \boldsymbol{K}_s^{(e)} K_r(\hat{\psi}^{(e)}) \frac{\boldsymbol{dN}^{(e)}}{\boldsymbol{dz}} dz \tag{18}$$

$$\boldsymbol{F}^{(e)} = \int_{\boldsymbol{\Omega}^{(e)}} C(\hat{\psi}^{(e)})\, \boldsymbol{N}^{(e)} (\boldsymbol{N}^{(e)})^T dz \tag{19}$$

Here, $\boldsymbol{N}^T$ denotes the transpose of $\boldsymbol{N}$.

3. LINEARIZATION METHODS

It is very challenging task to solve the equation (1) efficiently, because of strong nonlinearity due to pressure head dependencies in the specific moisture capacity and hydraulic conductivity. Hence iterative calculation and standard linearization techniques, such as Picard and Newton iterations methods are needed to solve. While a number of iterative schemes have been recommended [e.g. 10, 20, 21, 38]. Newton-Raphson methods converge quadratically yet they often be unsuccessful for parabolic degenerate case where the Jacobian matrix might become singular and because of poor initial solution estimate. On the other hand, Picard method is simple and exhibits a good performance in many problems [23, 38]. In this study, we have implemented these two most frequently used iteration approaches.

Newton Scheme

Let us Consider

$$\boldsymbol{f}(\boldsymbol{\Psi}^{k+1}) = \boldsymbol{A}\big(\boldsymbol{\Psi}^{k+\lambda}\big)\boldsymbol{\Psi}^{k+\lambda} + \boldsymbol{F}\big(\boldsymbol{\Psi}^{k+\lambda}\big)\frac{\boldsymbol{\Psi}^{k+1} - \boldsymbol{\Psi}^{k}}{\Delta \mathrm{t}^{\mathrm{k}+1}} - \boldsymbol{q}\big(t^{k+\lambda}\big) + \boldsymbol{b}\big(\boldsymbol{\Psi}^{k+\lambda}\big) = 0 \tag{21}$$

The Newton scheme [42] can be written as:

$$\boldsymbol{f}'\big(\boldsymbol{\psi}^{\boldsymbol{k}+\mathbf{1},(\boldsymbol{m})}\big)\big(\boldsymbol{\psi}^{\boldsymbol{k}+\mathbf{1},(\boldsymbol{m}+\mathbf{1})} - \boldsymbol{\psi}^{\boldsymbol{k}+\mathbf{1},(\boldsymbol{m})}\big) = -\boldsymbol{f}\big(\psi^{k+1,(m)}\big) \tag{22}$$

where the superscripts *m* and *m* + 1 denote the previous and current iteration levels.
The Jacobian for the system is:

$$f'_{ij} = \lambda A_{ij} + \frac{1}{\Delta t^{k+1}} F_{ij} + \sum_s \frac{\partial A_{is}}{\partial \psi_j^{k+1}} \psi_s^{k+\lambda} + \frac{1}{\Delta t^{k+1}} \sum_s \frac{\partial F_{is}}{\partial \psi_j^{k+1}} (\psi_s^{k+1} - \psi_s^k) + \frac{\partial b_i}{\partial \psi_j^{k+1}} \tag{23}$$

expressed here in terms of *ij*-th component of the Jacobian matrix $\boldsymbol{f}'(\boldsymbol{\Psi}^{k+1})$.

Picard Scheme

The Picard method is a straightforward formulation which can be derived from (20) by iterating with all linear occurrences of ψ^{k+1} taken at the current iteration level *m* + 1 and all nonlinear occurrences at the previous level *m*. We get:

$$\left[\lambda \boldsymbol{A}^{\boldsymbol{k}+\lambda,(m)} + \frac{1}{\Delta t^{k+1}} F^{k+\lambda,(m)}\right]\left(\boldsymbol{\psi}^{\boldsymbol{k}+\mathbf{1},(\boldsymbol{m}+\mathbf{1})} - \boldsymbol{\psi}^{\boldsymbol{k}+\mathbf{1},(\boldsymbol{m})}\right) = -\boldsymbol{f}\left(\psi^{k+1,(m)}\right) \tag{24}$$

Symmetric and nonsymmetric system matrix formed for the Newton and Picard linearization methods respectively and these two features are the influential factors to evaluate the relative competence of Picard and Newton schemes. Three derivative terms are needed to estimate in the Jacobian for Newton iteration method, hence computation cost is very high and more complex than Picard scheme.

4. METHODOLOGY

We have examined two regular iterative methods which can be applied in a solution strategy for the nonlinear Richards' equation governing flow in partially saturated porous medium. We started linear discretizations and linearization techniques which grant us to evade iterations in the numerical solution of Richards' equation. In this study, we have assessed the accuracy and computational efficiency of the iterative Newton and Picard strategies. The assessments are originated on various one-dimensional saturated-unsaturated test examples with homogeneous and heterogeneous soil properties. Moreover, to achieve accuracy and efficiency of the proposed method, we have also examined quickly different highlights of the systems including symmetry, stability criterions and mass balance errors. Numerical trials are executed with mass lumping, to judge the robustness of the technique and explore the leads of the procedure for enhancing the efficiency of solutions to Richards' equation. Moreover, spatial adaptation is employed based upon a fine grid discretization and temporal adaptation is accomplished using variable order, variable step size based upon the backward Euler finite difference formula.

A few strategies have been proposed to improve the presentation of the Picard and Newton techniques for situations where convergence difficulties are experienced. These methods which incorporate relaxation and chord slope differentiation are actualized alongside another mixed methodology including the utilization of Picard iteration to improve the initial solution estimate for the Newton scheme. Adaptive time stepping strategies can be easily incorporated into the Picard and Newton iterative schemes. The time steps will be adjustable consequently based on the quantity of iterations required for combination at the previous time step [39].

Dynamically adjusted time stepping strategies are included during simulation on the report of the convergence conduct of the nonlinear iteration approach. A convergence tolerance $Tol\ (= 10^{-4})$ is indicated, alongside a most extreme number of iterations for nonlinear solver $maxit$, allowed during whenever step. The simulation starts with a initial time step size, which is defined by user (denoted by Δt_0 in our study) and continues until reach the final time T_{max}. The present size of simulation step is expanded by a magnification factor ($\Delta t_{mag} = 1.20$) if nonlinear convergence is accomplished in less than maximum allowed iterations, it is left unaltered if convergence required between $maxit_1$ and another predefined iterations limit $maxit_2$, and it is decreased with a reduction factor $\Delta t_{red} = 0.5$ if solver needs more than $maxit_2$ iterations to attain convergence. In case convergence is not accomplished within the maximum number of iterations ($maxit$ exceeded), the solution at the current time level is recalculated (which is called "back stepping" of solver) utilizing a decreased time step size (i.e., factor Δt_{red} reduced to minimum step size Δt_{min}) or then again the first run through of a simulation, the initial conditions are applied as the first solution estimate for the iterative strategy. For resulting time steps of a simulation, the pressure head solution from the past step is considered as the first guess. Along these lines time step size directly affects convergence conduct, through its effect on the nature of the initial solution estimation. The convergence error of nonlinear iterative technique is evaluated by the relation $\left\|\boldsymbol{\psi}^{k+1,(m+1)} - \boldsymbol{\psi}^{k+1,(m)}\right\| \leq Tol$ and the residual error is computed using the l_∞ norm.

Analytical differentiation is used to evaluate the specific moisture capacity. Relaxation has been proposed as a method of upgrading convergence of nonlinear iterative approaches specifically when

oscillations in $\boldsymbol{\Psi}$ happen starting with one iteration then onto the next [39]. The current solution $\boldsymbol{\psi}^{k+1,(m+1)}$ is then updated to $\boldsymbol{\psi}^{*}$ by the relationship $\boldsymbol{\psi}^{*} = \boldsymbol{\Omega}\boldsymbol{\psi}^{k+1,(m+1)} + (1-\boldsymbol{\Omega})\boldsymbol{\psi}^{k+1,(m)}$ [36]. In the subsequent choice $\boldsymbol{\Omega}$ is steady, and the relaxation step can be identically communicated by multiplying the right-hand sides of the Newton expression (24) or the Picard expression (26) by $\boldsymbol{\Omega}$ [41].

One of the fundamental disadvantages of the Newton method used to be the inadequacy of linear solvers for large and sparse nonsymmetric systems. This is not true anymore, as of now accessible conjugate gradient-type methods for solving nonsymmetric systems have gotten progressively dependable and efficient. Biconjugate gradient stabilized algorithm, BICGSTAB is employed for solving our test examples. Incomplete Cholesky conjugate gradient technique, ICCG is used for solving the symmetric systems occurred from Picard linearization method. Convergence tolerance for linear solver is 10^{-10} and 1000 iterations are allowed to achieve convergence.

Our all simulations were performed with this one of the most stable, accurate, efficient and robust model catchment hydrology, (CATHY) which is a physically based hydrological model, couples a finite element solver for the Richards' equation describing flow in variably saturated porous media [38, 42] and a finite difference solver for the diffusion wave equation describing surface flow. All computations were performed on Dell XPS 15 9570 with an Intel Core i7-8750H CPU @ 2.20 GHz, 64-bit operating system, x64-based processor.

5. NUMERICAL TESTS AND RESULTS

So as to test and assess the performance of the solution algorithm plot over, the technique is applied to three illustrative one-dimensional sets of published experiments, each of which corresponds to different physical setting and contrasted with results accessible in the literature. The first one-dimensional test case deals with dry initial conditions and the steep wetting front develop and hence numerical simulation of this test is very difficult [17, 19]. This test case gave stringent test to the technique sketched in this study. The second one-dimensional experiment manages a sharp moisture front that infiltrates into the vertical soil column [20, 43, 44, 45]. The third experiment contains flow into a layered soil and a drainage case with variable initial conditions [43, 45, 46] involves flow into very dry heterogeneous soil. These test cases represent a diversity of media and a good challenge for a numerical procedure due to their highly nonlinear nature.

Test Case 1

This problem considers a vertical soil column whose length is $10\ m$. The pressure head distribution is initially dry with a water table boundary condition $\psi(0,t) = 0$ is imposed at the bottom and a saturated boundary condition $\psi(10,t) = 0.1$ is applied on the top of soil column. The material properties for this test problem correspond to dune sand. The soil parameters are $\theta_s = 0.301$, $\theta_r = 0.093$, $\alpha = 5.47/\mathrm{m}$, $n = 4.264$ and $K_s = 5.040\ \mathrm{m/day}$. The soil hydraulic properties are described by the van Genuchten model and the typical nature of soil characteristics curves are made Richards' equation highly nonlinear.

Clearly it is evident that the set of simulation condition yield a difficult sharp-front problem. This test case is considered on the grounds that it suggests a phenomenal benchmark problem permitting us to examine methods for quantifying the accuracy, efficiency and robustness of the resultant solutions. The large computational domain and saturated condition combined propose that this test case is very complex sharp-front problem and will give a rigorous and meaningful test issue for evaluation the solution approaches.

Numerical simulation for this classical test case is performed with two set of fine spatial grid discretizations (401 and 801 nodes i.e., $\Delta z = 0.025\mathrm{m}$ and $0.0125\ \mathrm{m}$). Each set of grid size is used along with three maximum step sizes $\Delta t_{max} = 10s, 100s$ and $1000s$ and three iterations limits are $maxit = 10, maxit_1 = 8$ and $maxit_2 = 5$. The computed oscillation-free pressure head profiles after 0.20 days for Picard and Newton iterations are depicted by Figure 1 and the results are completely agreed with the published solution [17, 19]. It is noted that, the solution profiles are quiet agreed with each other for both the linearization techniques. Furthermore, sharp-front with saturation conditions are developed and drained-to-equilibrium initial condition is easily noted.

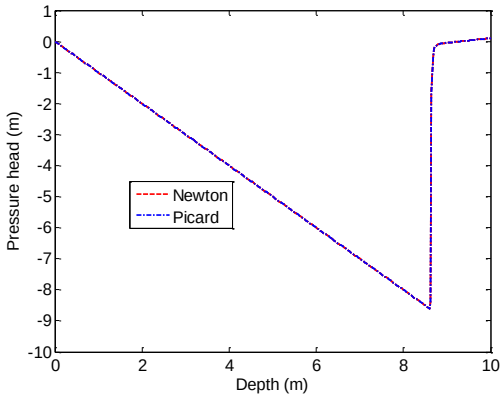

Figure 1. Pressure head profiles for Picard and Newton methods for Test Case 1.

To analysis the performance of Picard and Newton iterations methods on the basis of other aspects of the flow equation, we computed step size behavior (Figure 2), number of nonlinear iterations per time step (Figure 3) and cumulative mass balance errors (CMBE) (Figure 4) for $\Delta t_{max} = 10s, 100s \text{ and } 1000s$.

For the case of $401 \text{ and } 801$ nodes, Picard and Newton methods for all time step sizes are showing same behavior. Time stepping is decreasing with increasing the number of nodes for Picard scheme, whereas, Newton shows the reverse nature for all the temporal discretizations. Picard method faces severe convergence difficulties for 801 nodes throughout the entire simulation but for less complexity are noted 401 nodes. Time step size will increase with increase the number of nodes for Newton scheme and lesser difficulties are shown to achieve the convergence. Hence it is not necessary that to increase the maximum size of time because both solvers never achieve their maximum step size.

Number of nonlinear iterations for achieving convergence when Picard and Newton iteration methods are used for all spatial and temporal cases and are plotted in the Figure 3. Picard method demonstrates almost similar conduct for 401 and 801 nodes for three time step sizes and it is true also for Newton scheme. Initially much number of iterations are required to attain convergence for both techniques. Convergence problems are increasing with the number of nodes for both algorithms due to sharp-front of the moisture soil. This is an important nature since it is influencing the iteration efficiency of the numerical solver. The iteration numbers are needed in Newton and Picard methods are almost same for all cases. These represent a comparison of the dense (401 nodes) and very dense (801 nodes) solutions to illustrate the spatial discretization consequence. Mass balance error is another important factor for solution accuracy. Pressure head form of Richards' equation produces poor mass balance due to the involvement of the analytical moisture capacity function. Figure 4 shows the mass balance error profiles of the Picard and Newton schemes for two spatial discretizations (401 nodes and 801 nodes) of three time stepping. The degree of the errors is remarkably acceptable throughout the entire simulation, confirming to the consistency of the approximation and the reliability of the solution method. In all cases, similar error profiles were obtained, attesting the robustness of the adaptive time stepping technique for Picard and Newton methods with respect to the spatial discretization.

The accuracy, efficiency and robustness of the method can be measured based on various features, such as, number of time steps to complete the simulation, linear and nonlinear convergence behavior for each time step, number of back stepping of the solver, cumulative mass balance error, computational cost, etc. The total number of iterations can be utilized as the proportion of computational exertion since the CPU time is represented by the total number of matrix inversion, as opposed to by the quantity of time steps. Each run of Picard and Newton iterations of the finite element model with adaptive scheme is almost indistinguishable to other run.

Simulation performance of the Picard and Newton methods are presented in the Tables 1 and 2. It is obvious from Tables 1 and 2 that the Picard implementation is shown few simulation advantages than Newton method on the account of number of time steps for 401 nodes case but reverse solutions performance are exhibited for 801 nodes by Newton iteration solver. In fact, on the basis of other computational factors, the numerical performance of the Picard scheme is roughly equivalent to the Newton

scheme. This can be expected from the results, since the actual approximation formulae are identical and the procedures fluctuate only in the derivative terms are involved with Newton scheme. Also, note that similar mass balance error profiles imply similar time step histories and hence similar efficiency. The results presented here, the only effect that both iterative methods have, is on the convergence rates and computational efficiency. Thus the MBE or other errors cannot improve by choosing a different spatial discretization for any iterative methods.

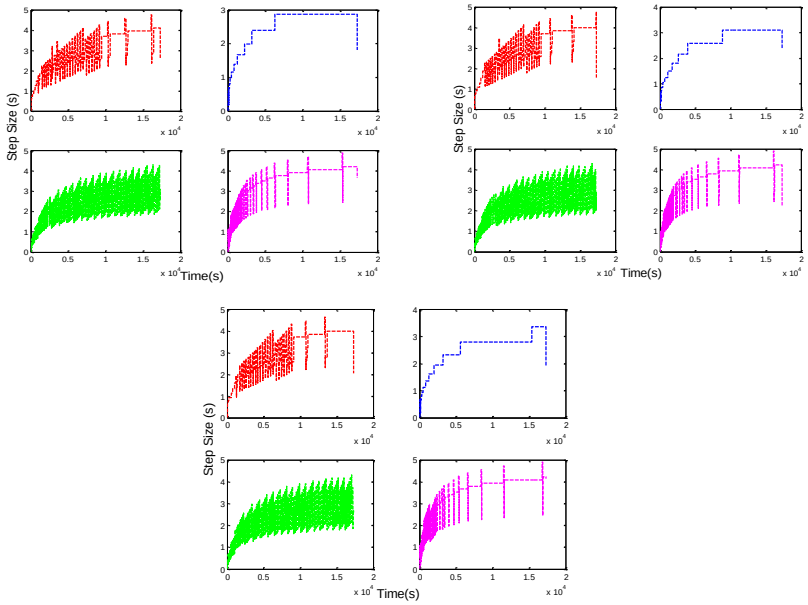

Figure 2. Time stepping behavior of Picard (left columns) and Newton (right columns) methods of 401 nodes (top rows) and 801 nodes (bottom rows) for $\Delta t_{max} = 10\ s, 100\ s$ and $1000s$ respectively for Test Case 1.

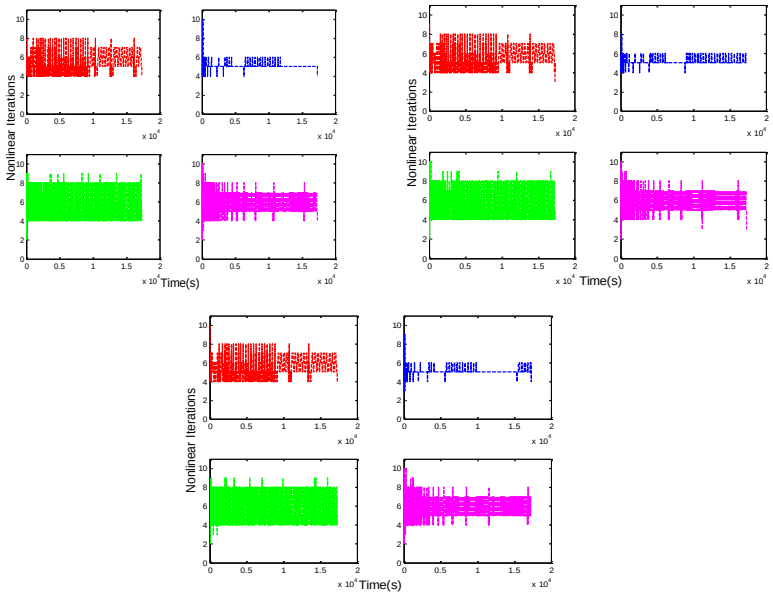

Figure 3. Nonlinear convergence behavior of Picard (left columns) and Newton (right columns) methods of 401 nodes (top rows) and 801 nodes (bottom rows) for $\Delta t_{max} = 10\ s, 100\ s$ and $1000s$ respectively for Test Case 1.

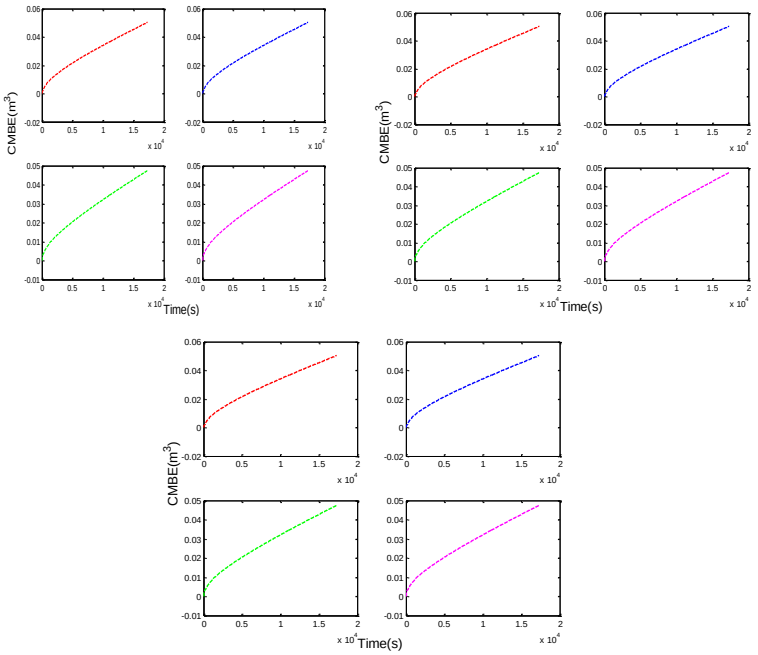

Figure 4. Mass balance error behavior of Picard (left columns) and Newton (right columns) methods of 401 nodes (top rows) and 801 nodes (bottom rows) for $\Delta t_{max} = 10\ s, 100\ s$ and $100\ s$ respectively for Test Case 1.

Table 1. Simulation statistics of Picard and Newton methods for 401 nodes for Test Case 1.

$\Delta t_{max}(s)$	10		100		1000	
Method	Pic	New	Pic	New	Pic	New
Total. No. of Time steps	6641	7641	6620	7467	6572	7647
Smallest step size (s)	1.192e-6	1.192e-6	1.490e-6	7.451e-7	1.863e-6	9.313e-7
Largest step size (s)	4.745e+0	2.870e+0	4.767e+0	3.100e+0	4.619e+0	3.348e+0
Avg. step size (s)	4.745e+0	2.261e+0	2.610e+0	2.341e+0	2.629eè0	2.260e+0
Avg. NLI/Step	5.51	5.09	5.53	5.15	5.58	5.11
Avg. LI/Step	33.95	30.98	34.03	31.25	34.30	30.98
No. of back steps	22	23	25	26	28	29
No. of linear solver failure	0	0	0	0	0	0
CMBE (m^3)	5.022e-2	5.0218e-2	5.0219e-2	5.0218e-2	5.028e-2	5.022e-2
CPU (s)	4922.04	8728.10	4725.33	8586.03	9929.85	14760

** No.=Number, Pic=Picard, New=Newton, NLI=Nonlinear iteration, LI=Linear iteration, Avg.=Average, CMBE=Cumulative mass balance error.

Table 2. Simulation statistics of Picard and Newton methods for 801 nodes for Test Case 1.

$\Delta t_{max}(s)$	10		100		1000	
Method	Pic	New	Pic	New	Pic	New
Total. No. of time steps	8154	5502	8126	5513	8160	5486
Smallest step size (s)	5.960e-7	2.980e-7	3.725e-7	3.725e-7	4.657e-7	4.657e-7
Largest step size (s)	4.280e+0	4.864e+0	4.293e+0	4.886e+0	4.306e+0	4.901e+0
Avg. step size (s)	2.119e+0	3.141e+0	2.127e+0	3.134e+0	2.118e+0	3.150e+0
Avg. NLI/Step	5.25	5.42	5.28	5.43	5.25	5.44
Avg. LI/Step	31.57	36.70	31.71	36.62	31.59	36.75
No. of back steps	24	38	27	43	30	44
No. of linear solver failure	0	0	0	0	0	0
CMBE (m^3)	4.733e-2	4.735e-2	4.735e-2	4.735e-2	4.733e-2	4.735e-2
CPU (s)	12358	14031.55	13476.92	31291.54	15569.37	14270.02

Test Case 2

Comparison between Picard and Newton schemes is performed on the test case of $2\ m$ soil column, which discretized with two fine vertical resolutions $\Delta z = 0.008\ m$ and $0.004\ m$ (i.e., 251 and 501 nodes). The initial pressure head distribution is $\psi(z,0) = z - 2$. The bottom of the boundary condition is water table boundary condition (i.e., $\psi(0,t) = 0$)), while a time-dependent Dirichilet boundary condition

$$\psi(2,t) = \begin{cases} -0.05 + 0.03\sin\left(\frac{2\pi t}{100000}\right) & if\ 0 < t \leq 100000 \\ 0.1 & if\ 100000 < t \leq 180000 \\ -0.05 + 2952.45\, e^{-\frac{t}{18204.8}} & if\ 180000 < t \leq 300000 \end{cases}$$

is applied at the top boundary. The soil hydraulic parameters are $\theta_s = 0.410$, $\theta_r = 0.095$, $\alpha = 1.9/\mathrm{m}$, $\mathrm{n} = 1.31$ and $\mathrm{K_s} = 0.062\ \mathrm{m/day}$. Van Genuchten's soil water retention model is used to simulate this test problem. These forcing conditions lead to a challenging problem, further it corresponds to a sharp-front infiltration and produce large gradients in the solution. Such kind of test case gives a rigorous test problem for any numerical solver and is well fitted to compare the computational performance of the iterative nonlinear solvers. The soil water retention curves are monotonic with a point of inflection that gives the moisture capacity function its classic behavior. The soil moisture properties are described by the van Genuchten model.

A group of simulations was performed to compare the performance of two iterative methods. Simulations for this test problem is performed using three different set of maximum allowable time step size (i.e., $\Delta t_{max} = 10s, 100s$ and $1000s$), and three types of nonlinear iteration limits are $maxit = 15$, $maxit_1 = 10$ and $maxit_2 = 6$. The evaluated pressure head profiles of 501 nodes for both iteration techniques at different times are presented by the Figure 5. Computed solutions from Picard and Newton methods are quiet similar to published studies [20, 43, 44, 47].

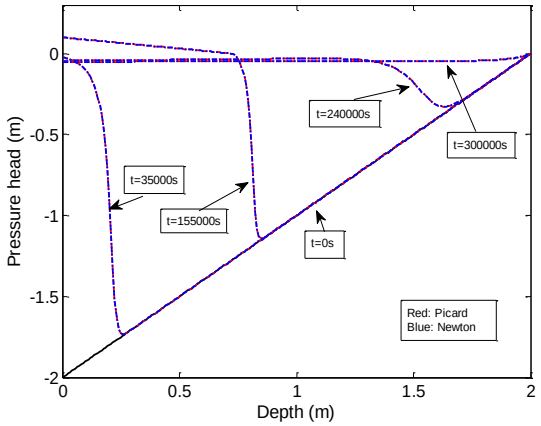

Figure 5. Pressure head profiles for Picard and Newton methods for Test Case 2.

It is clear that the second time interval of the simulation (100 000 < t ≤ 180 000) is viewed as extremely trying for numerical integrators. The unexpected increment of the upper Dirichlet boundary condition to a positive estimation of 0.1m (ponding) produces a sharp moisture front that infiltrates into the soil column. Toward the start of the third time span (t > 180 000 s) ponding diminishes exponentially, arriving at asymptotically a last estimation of −0.05m, and before the finish of the simulation the whole soil column is near full saturation.

Dynamic time stepping conducts (Figure 6) of Picard and Newton techniques for all vertical discretizations with different maximum permissible step size measures are examined in the numerical evaluation of Richards' equation. We discovered generally striking here the altogether different nature between the Newton and Picard strategies during the ponding time frame. It is evident that toward the finish of first interval of simulation time, enormous time steps are accomplished, yet these drop drastically in the time period $100000s \leq t \leq 200000s$ to attain the convergence of Picard solver for all cases. In this ponding period a slight expanding pattern in time step size can all things considered be watched, strong oscillations moreover happen. These oscillations have been credited to deficient spatial resolutions. The time step size stays little from 100 000s to 200 000s, as ponding slowly diminishes to zero. But in the Newton solver case, very few convergence difficulties are observed at $100000s$ and $200000s$ for 251 nodes with all allowable maximum step sizes. Also, note that Newton iteration method is completely divergent for $\Delta t_{max} = 100s$ and $1000s$ of $\Delta z = 0.002m$ vertical resolution. In the last period of simulation time $200000s \leq t \leq 300000s$ builds quickly and arrives at maximum permissible step size for all cases of Picard and Newton schemes. This demonstrates simpler nonlinear solver conditions because of smoother infiltration fronts and surface conditions that are not, at this point completely saturated. Obliging an iteration procedure to make very little time steps for delayed periods during a simulation can speak to a monstrous computational difficulty for subsurface solvers.

Graphical portrayal of convergence performance regarding number of the nonlinear iterations demanded at each step of Picard and Newton iterative approaches are appeared in the Figure 7. According to these graphs, we point that a smoother change into and out of the ponding time cycle, and without the requirement for time step adjustment. On the other time domain, Picard integrator needs to negotiate a wide range of iteration up to maximum tolerable iteration limits to converge for all spatial and temporal resolutions. In the Newton plot, we found that very smooth convergences are achieved with $\Delta t_{max} = 10\ s$ for both grids spacing except other temporal discretizations. Therefore, it demonstrates that small step size is influential for efficient numerical solution.

In order to assess the solution accuracy, the CMBEs of the solution through the domain are presented in the Figure 8. In the Picard and Newton runs for all cases, the MBE remains practically consistent and near to zero, confirming that the obtained solutions are quite adequate.

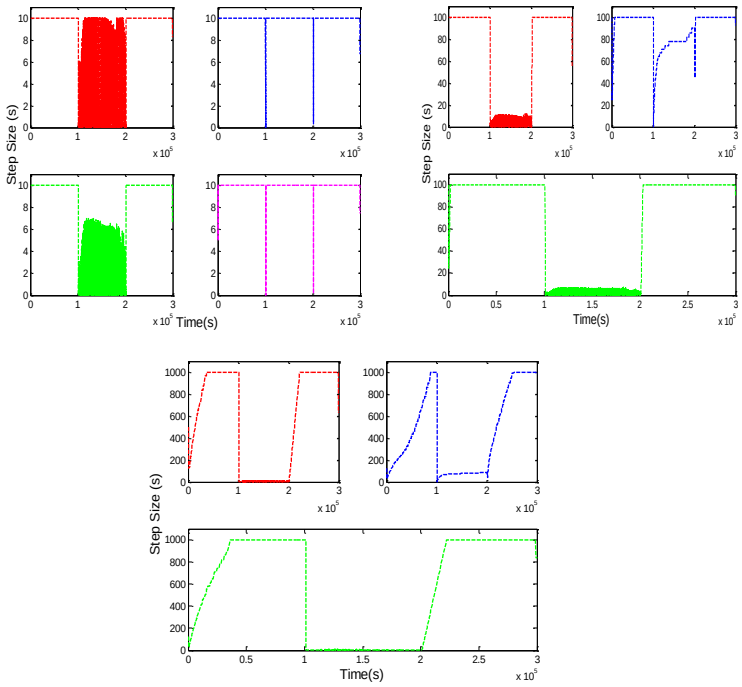

Figure 6. Time stepping behavior of Picard (left columns) and Newton (right columns) methods of 251 nodes (top rows) and 501 nodes (bottom rows) for $\Delta t_{max} = 10\ s, 100\ s$ and $100\ s$ respectively for Test Case 2.

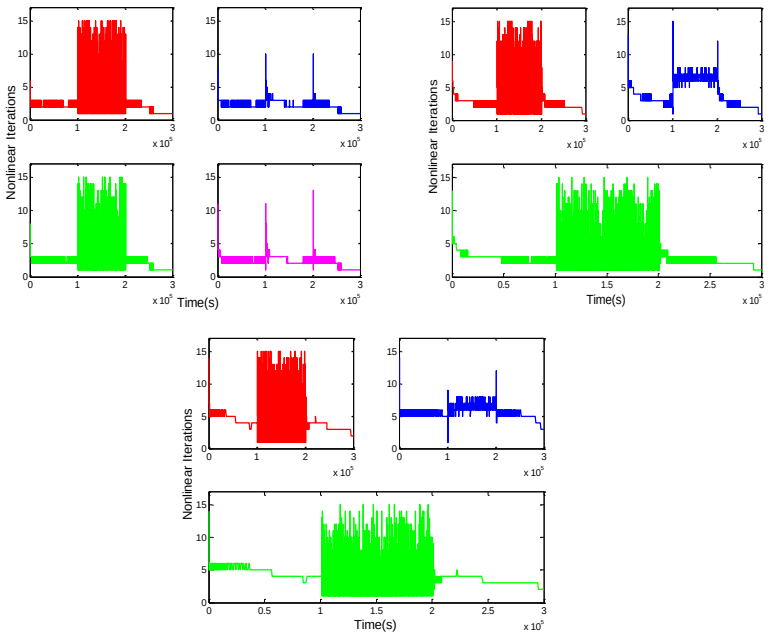

Figure 7. Nonlinear convergence behavior of Picard (left columns) and Newton (right columns) methods of 251 nodes (top rows) and 501 nodes (bottom rows) for $\Delta t_{max} = 10\ s, 100\ s$ and $1000\ s$ respectively for Test Case 2.

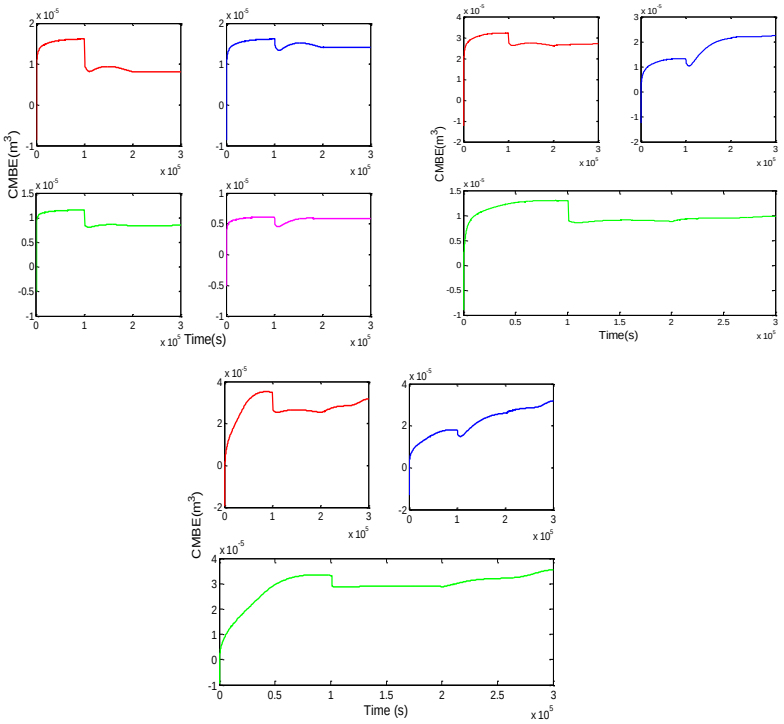

Figure 8. Mass balance error behavior of Picard (left columns) and Newton (right columns) methods of 251 nodes (top rows) and 501 nodes (bottom rows) for $\Delta t_{max} = 10\ s, 100\ s$ and $1000\ s$ respectively for Test Case 2.

Other reproduction insights are summed up in Tables 3 and 4, demonstrated the computational efficiency of Picard and Newton on the basis of number of iterations, stepping criteria, average nonlinear convergence nature CMBE, back stepping and CPU. The total number of time steps applied by Newton method are 4.5 times, 32.30 times and 53.18 times fewer than Picard scheme for $\Delta t_{max} = 10\ s, 100s$ and $1000s$ respectively for 251 nodes. Looking at all the more intently the computational performance of Picard and Newton iterations, we note that Newton runs came about in essentially lesser back-stepping events (such as, 16, 12, 22) than Picard runs (such as, 7937, 8066, and 8064) for all types temporal spacing for 251 nodes. The purpose behind this is the step sizes anticipated by dynamic time stepping control, while guaranteeing low truncation error, don't ensure convergence of the Picard strategy. In the event that the nonlinear solver doesn't converge within the maximum iteration limits, the back-stepping system is initiated whereby the current time step is reiterated with a reduced time step. This little Δt may bring about a low truncation error, setting the adaptive time stepping amplification factor for ascertaining whenever step size, quite often equivalent to its greatest estimation of Δt_{max}. Because of this unexpected increment in Δt, the Picard technique will most likely again not converge, and the back-stepping instrument is initiated once more. Another focus can be featured from the outcomes appeared in Table 3, e.g., the best CPU times are gotten for the least forceful time stepping techniques for Newton method and they are about 2.8 to 10.30 times fewer than Picard scheme.

Under profoundly nonlinear conditions, intermingling clearly requires time step measures that are a lot littler than those directed by accuracy contemplations alone. This recommends time step adjustment dependent on error control may not be ideal. A blended type of time step adjustment may subsequently be the best methodology, giving more weight to mixed based control when nonlinearities are gentle, and to nonlinear assembly conduct in any case. Surely successful models for solving nonlinear equations fundamentally cooperate with the time step size determination method. A complete methodology should utilize all the data that can be accumulated from the whole simulation. Enhancement strategies along with perfect control hypothesis give in this sense a perfect system for the solution.

Picard performance shows convergence achieved with very little average time step, the explanation being that the nonlinearities are not all that huge during the first period of simulation time and the simulation is constrained when truncation error. As a result, the amplification factors determined by the time stepping strategy never achieve their maximum allowable time step. In the wake of changing to ponding, be that as it may, the nonlinearity firmly increments and time step sizes should be maintained little in control to accomplish convergence of the Picard iteration method. These little time steps produce exceptionally little time truncation errors, bringing about maximal time step projections. The outcome is an unequivocally wavering time step size between the qualities forced by convergence necessities and those recommended by truncation error approximations, as can be obviously found in Figure 6.

The CMBE at any given time step is determined as the outright distinction between the adjustments in water stockpiling during that time step. The adjustment in water stockpiling is determined in two different ways, as the contrast between approaching and active water volumes and from changes in volumetric moisture content caused by contrasts in pressure head between the current and the past time level. Both Picard and Newton schemes are conserved perfect mass balance for runs.

Same computational statistics are observed from the Tables 3 and 4 for Picard and Newton methods, however Newton solver fail to attain convergence for large $\Delta t_{max} = 100s$ and $1000s$. The reason is the algebraic complexity, nature soil hydraulic properties, boundary conditions and derivative terms of the Jacobian matrix. Since we are interested to compare the accuracy and efficiency between Picard and Newton methods, 251 nodes is fine enough to ensure accurate solution. Extremely fine grid discretizations incurred large CPU costs. On the basis of all efficiency criterion, Newton scheme is superior to Picard scheme for solving such flow model.

Table 3. Simulation statistics of Picard and Newton methods for 251 nodes for Test Case 2.

$\Delta t_{max}(s)$	10		100		1000	
Method	Pic	New	Pic	New	Pic	New
Total. No. of time steps	136849	30247	120724	3737	118964	2237
Smallest step size (s)	9.329e-3	2.748e-2	1.051e-2	4.834e-2	9.586e-3	3.817e-2
Largest step size (s)	1.000e+1	1.000e+1	1.000e+2	1.000e+2	1.000e+3	1.000e+3
Avg. step size (s)	2.192e+0	9.918e+0	2.485e+0	8.028e+2	2.522e+0	1.341e+2
Avg. NLI/Step	2.44	2.05	2.55	4.26	2.56	5.93
Avg. LI/Step	10.70	9.89	11.95	29.24	12.05	47.55
No. of back steps	7937	16	8066	12	8064	22
No. of linear solver failure	0	2	0	1	0	3
CMBE (m^3)	8.119e-6	4.405e-5	2.701e-5	2.240e-5	3.177e-5	3.191e-5
CPU (s)	22816.65	7905.88	19176.71	2365.70	18758.48	1820.65

Table 4. Simulation statistics of Picard and Newton methods for 501 nodes for Test Case 2.

$\Delta t_{max}(s)$	10		100		1000	
Method	Pic	New	Pic	New	Pic	New
Total. No. of time steps	186041	30255	166926	DIV	164982	DIV
Smallest step size (s)	5.426e-3	1.591e-2	7.417e-3		7.682e-3	

Largest step size (s)	1.000e+1	1.000e+1	1.000e+2	E R G E N T	1.000e+3	E R G E N T
Avg. step size (s)	1.613e+0	9.912e+0	1.797e+0		1.818e+0	
Avg. NLI/Step	2.37	2.08	2.44		2.44	
Avg. LI/Step	9.53	10.28	10.42		10.49	
No. of back steps	11408	14	11330		11330	
No. of linear solver failure	0	1	0		0	
CMBE (m^3)	8.435e-5	5.901e-6	9.844e-6		3.549e-5	
CPU (s)	54233.05	15764.47	49380.52		51137.68	

Test Case 3

This case involves vertical drainage through layered soil from initially saturated conditions. At time$t = 0$, the pressure head at the base of the column is reduced from 2 to $0\,m$. During the subsequent drainage, a no-flow boundary condition is applied to the top of the column. Although a one-dimensional test case, it is a difficult test for a numerical technique as a result of the sharp discontinue in the moisture content that happens at the interface between two material layers.

During drain-down the middle coarse soil tends to restrict drainage from the upper fine soil and high saturation levels are maintained in the upper fine soil for a considerable period of time. The soil hydraulic properties are described in Table 5. The Brooks–Corey model is applied to estimate pressure–moisture relationship. The soil profile for soil 1 is $0\,m < z < 0.6\,m$ and $1.2\,m < z < 2\,m$ and soil 2 for $0.6\,m < z < 1.2\,m$, where z is the vertical length of the soil column.

Table 5. Soil hydraulic properties used in Test Case 3.

Parameters	Soil 1	Soil 2
θ_s	0.35	0.35
θ_r	0.07	0.035
$\alpha\ (\mathrm{cm}^{-1})$	0.0286	0.0667
n	1.5	3.0
$K_s\ (\mathrm{cm/s})$	9.81×10^{-5}	9.81×10^{-3}

Brooks–Corey model is used to recommend the soil moisture relations. The state of the soil moisture specific capacity for both soils materials is very sharp close to saturation infers the thorough complexities are experienced when the analytical differentiation of fluid content is used. Therefore, numerical solutions are severely influenced. To deal with such challenge effectively, legitimate decision of grid and temporal resolution, as well as, efficient numerical integrators is needed for heterogeneous permeable media.

Simulations were executed on a fine grid resolution (150 elements) and a very fine grid resolution (300 elements). As our knowledge, such difficult problem is solved with 150 elements, which is much more sufficient to obtain accurate and efficient numerical solution. We used three different group of maximum allowable time step size (i.e., $\Delta t_{max} = 10s, 100s$ and $1000s$), and three types of nonlinear iteration limits are $maxit = 10$, $maxit_1 = 8$ and $maxit_2 = 6$ for both Picard and Newton iteration schemes. The iterative methodology inside a period step was considered merged when the discrete in the water pressure head between two consecutive iterations fell beneath 10^{-3}. Figure 9 shows the water saturation predictions alongside the Picard and Newton iterative solution during a period of $1050000\ s$ (roughly 12 days) with 301 nodes. There is excellent agreement between the computed solutions obtained using Picard and Newton methods and also published studies [43, 45, 46]. These profiles are clearly illustrating apparently accurate, convergent and efficient solution.

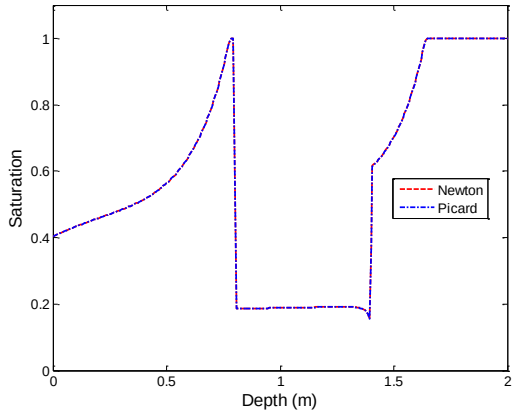

Figure 9. Saturation predictions after approximately 12 days of Picard and Newton methods for Test Case 3.

The evolution of step size characterized by Picard and Newton methods are quite different (Figure 10) for all cases. It is found that Picard scheme needs small time steps to achieve convergence and remaining simulations are completed with its maximum step size $10\ s$. Little convergence is shown at $2 \times 10^5\ s$ in the Picard run for other two temporal step sizes. On the other hand, the excess oscillation patterns are appeared in the all Newton runs. Newton scheme is able to reach its maximum step up to $2 \times 10^5\ s$. During the remainder time of simulation, the numerical result applying Newton method had strong trouble converging, as demonstrated by the slower convergence and is required to reduce step size to obtain convergence. This trend continuously increases for $\Delta t_{max} = 100\ s$ and $1000\ s$ for both grid spacing. Figure 11 is demonstrated the results of nonlinear iterations for achieving convergence, showing that Picard technique have better iteration efficiencies. We have found that the number of nonlinear Picard iterations remained roughly 1 or 2, whereas, Newton method is used maximum iterations limit for all cases. Iteration efficiency cannot accelerate with decreasing the step sizes in Newton runs. That is, the difficult hydrologic responses are not resolved with fine vertical resolution due to probably the effects of soil heterogeneities. It is expected since in the Newton method, Jacobian evaluation is required at each time step. Nonlinear iterations plots are demonstrated that Newton iteration efficiency is inferior to Picard. The plots of simulated CMBE by Picard and Newton methods against time are presented in the Figure 12. Similar CMBE results are obtained for each of the simulations. The value of the CMBE with different time step sizes for all grid resolutions are significantly lower (e.g., the values are less than 2×10^{-6}, 8×10^{-6} and 2×10^{-5} for $\Delta t_{max} = 10\ s, 100\ s$ and $1000\ s$ cases respectively for 150 and 300 elements). Computed results are confirming the conservation of good mass balance of the both iteration techniques.

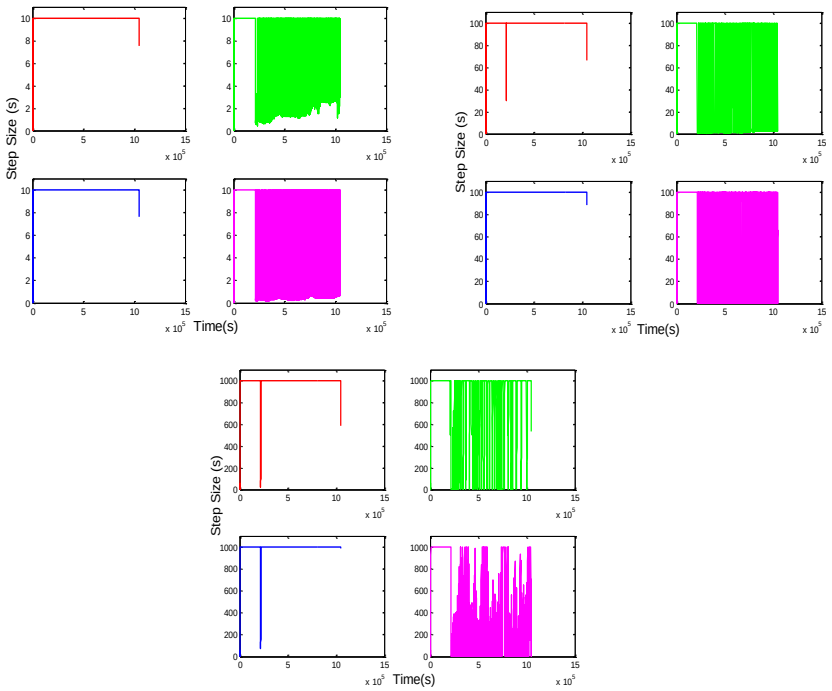

Figure 10. Time stepping behavior of Picard (left columns) and Newton (right columns) methods of 151 nodes (top rows) and 301 nodes (bottom rows) for $\Delta t_{max} = 10\ s, 100\ s$ and $1000\ s$ respectively for Test Case 3.

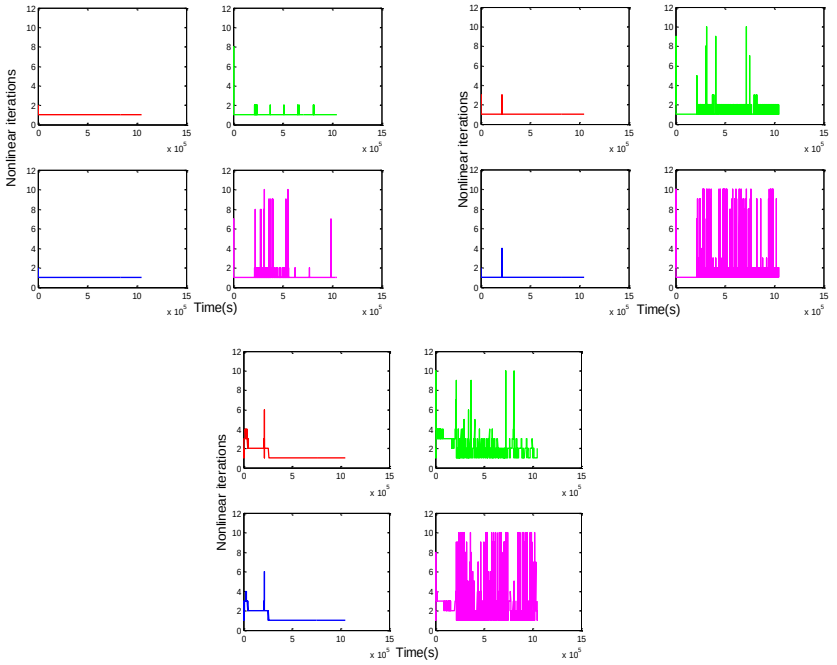

Figure 11. Nonlinear convergence behavior of Picard (left columns) and Newton (right columns) methods of 151 nodes (top rows) and 301 (bottom rows) for $\Delta t_{max} = 10\ s, 100\ s$ and $1000\ s$ respectively for Test Case 3.

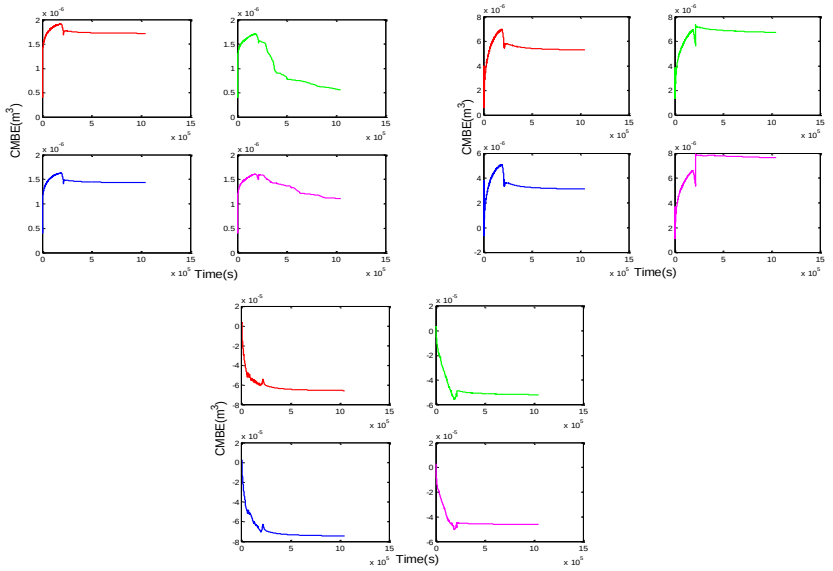

Figure 12. Mass balance error behavior of Picard (left columns) and Newton (right columns) methods of 151 nodes (top rows) and 301 nodes (bottom rows) for $\Delta t_{max} = 10\ s, 100\ s$ and $1000\ s$ respectively for Test Case 3.

Tables 6 and 7 are listed the comparison of simulated computational efforts of Picard and Newton schemes. The simulation performances are quiet similar among the results using Picard scheme. We have observed that there are large differences between Picard and Newton methods on account of total number of time steps. Newton iteration method needs larger number of steps to complete simulation than Picard for all cases. The differences in feature nonlinear behavior of all Picard runs not have considerable effects on the numerical performance of the model with increasing the grids. In each case, to attain convergence, all runs of Newton are needed about 3-4 nonlinear iterations and convergence of the linear solver is slower than Picard scheme during the simulation (approximately 50-60 iterations). All simulations by Newton method are successfully completed but all of runs encountered complexities rigorous enough to require many back stepping. Other main difference in numerical performance between the both techniques is that the simulation using Newton required significantly more CPU time than Picard. In fact, the computed results presented in the Tables 6 and 7 are very reasonable.

Table 6. Simulation statistics of Picard and Newton methods for 151 nodes for Test Case 3.

$\Delta t_{max}(s)$	10		100		1000	
Method	Pic	New	Pic	New	Pic	New
Total. No. of time steps	105051	243071	10558	85175	1201	52030
Smallest step size (s)	3.375e-2	7.031e-3	3.516e-2	2.109e-2	3.797e-2	2.373e-3
Largest step size (s)	1.000e+1	1.000e+1	1.000e+2	1.000e+2	1.000e+3	1.000e+3
Avg. step size (s)	9.995e+0	4.320e+0	9.945e+1	1.233e+1	8.743e+2	2.018e+1
Avg. NLI/Step	1.00	3.08	1.03	3.39	1.97	3.62
Avg. LI/Step	6.55	64.61	7.77	56.86	19.35	51.63
No. of back steps	15	50523	17	20245	59	13477

No. of linear solver failure	0	170	0	85	0	112
CMBE (m^3)	1.607e-6	5.559e-7	3.37e-6	6.709e-6	-7.858e-5	-5.145e-5
CPU (s)	3593.89	75983.48	371.10	25795.25	85.59	16396.93

Table 7. Simulation statistics of Picard and Newton methods for 301 nodes for Test Case 3.

$\Delta t_{max}(s)$	10		100		1000	
Method	Pic	New	Pic	New	Pic	New
Total. No. of time steps	105051	380694	10560	143872	1236	95730
Smallest step size (s)	3.375e-2	3.516e-3	2.531e-2	9.155e-4	3.164e-2	9.492e-3
Largest step size (s)	1.000eè3	1.000e+1	1.000e+2	1.000e+2	1.000e+3	1.000e+3
Avg. step size (s)	9.995e+0	2.758e+0	9.943e+1	7.298e+0	8.495e+2	1.097e+1
Avg. NLI/Step	1.00	3.13	1.03	3.53	2.02	3.65
Avg. LI/Step	6.55	53.12	7.74	57.69	19.54	57.66
No. of back steps	15	81169	17	36050	68	25014
No. of linear solver failure	0	301	0	202	0	132
CMBE (m^3)	1.607e-6	1.102e-6	3.238e-6	7.635e-6	-8.602e-5	-4.613e-5
CPU (s)	3593.89	210042.33	744.87	88145.09	176.77	60980.04

6. CONCLUSIONS

Appropriate numerical models for solving nonlinear flow problems are computationally serious and improved standard algorithms are needed that can simulate efficiently, accurately and robustly. Efficiency guarantees perfect usage of CPU and capacity assets to accomplish an ideal degree of solution exactness, while strength infers that a given procedure shows satisfactory convergence conduct over a wide range of simulation frameworks. The two most usually employed iterative systems for solving pressure Head-based Richards' equation, the Picard and Newton strategies, have been tried in a series of finite element simulations of flow in dynamically saturated permeable media. Numerical outcomes were looked at Picard and Newton solution, just as with a numerical result generated with a very fine spatial resolution. Dry initial conditions with steep wetting front, sharp moisture front that infiltrates into soil column and flow into a layered soil with variable initial conditions in one-dimensional media were led. Different components influencing the efficiency and strength of the Picard and Newton strategies were researched. These components are shown and their belongings outlined and summed up in the tables and figures for every one of the experiments. For the third test case, the Picard conspire converges well, and in such case it is obviously seen as more effective technique for linearizing Richards' equation than the Newton technique simulating vertical drainage problem through heterogeneous soil with saturated initial conditions. The best outcomes in term of accuracy and CPU time were obtained with the Picard structure. Conversely, calculation of the Jacobian by irritation required more CPU time than its analytical calculation for Newton. The Newton method is commonly more powerful and faster converging than Picard, despite the fact that it also can neglect to converge for enormous step size in layered soil case because of emphatically nonlinear characteristic equations and

discontinuities between material interfaces. For solving the Richards equation with a variable time step, Newton's technique required less CPU time than the Picard strategy, when simulating infiltration in an initially dry porous medium. However, for other two test cases, the Picard scheme converges very slowly. We note specifically the challenges experienced with gravity when simulating infiltration in an initially dry porous medium. In future work the impacts of two or three-dimensional flow cases on convergence conduct not tended to in this project, will be researched.

ACKNOWLEDGMENTS

We acknowledge the financial support of the SUST Research Center, Shahjalal University of Science & Technology, Sylhet (Project Code: PS/2018/2/21), Bangladesh.

References

[1] Marinelli, F. and Durnford, D.S.: *Semi analytical solution to Richards equation for layered porous media.* J. Irrigation and Drainage Eng., 1998, **124**:290 –299.
[2] Arampatzis, G.; Tzimopoulos, C.; Sakellariou-Makrantonaki, M.; Yannopoulos, S.:*Estimation of unsaturated flow in layered soils with the finite control volume method.* Irrigation and Drainage, 2001, **50(4)**, 349–358.
[3] Miller, C.T.; Abhishek, C.; Farthing, M.W.: *A spatially and temporally adaptive solution of Richards' equation*. Adv. Water Resour., 2005, ***29***:525–545.
[4] Richards, L.A.: *Capillary conduction of liquids through porous mediums*. Physics, 1931, **1(5)**: 318–333.
[5] Celia, M. A., Bouloutas, E. T., and Zarba, R. L.: *A General mass-conservative numerical solution for the unsaturated flow equation*, Water Resour. Res., 1990, **26(7):**1483-1496.
[6] Miller, C. T., Williams, G. A., Kelly, C. T., and Tocci, M. D.: *Robust solution of Richards' equation for non uniform porous media.* Water Resour. Res., 1998, **34**:2599-2610.
[7] Celia, M. A. and Binning, P.: *A mass conservative numerical solution for two-phase flow in porous media with application to unsaturated flow*. Water Resour. Res., 1992, **28(10)**: 281-928.
[8] Kees, C. E., and Miller, C. T.: *Higher order time integration methods for two-phase flow*. Adv. Water Resour 2002, **25(2)**:159–77.
[9] Chavent G. and Roberts, J. E.: *A unified physical presentation of mixed, mixed-hybrid finite elements and standard finite difference approximations for the determination of velocities in water flow problems.* Adv Water Resour., 1991, **14(6)**:329–348.
[10] Bergamaschi, L., and Putti, M.: *Mixed finite elements and Newton-type linearizations for the solution of Richards' equation.* Int. J. Numer. Methods Eng., 1999, **45**:1025-1046.
[11] Farthing, M. W., Kees, C. E. and Miller, C. T.: *Mixed finite element methods and higher-order temporal approximations.* Adv Water Resour., 2002, **25(1)**:85–101.
[12] Huyakorn, P. S., and Pinder, G. F.: *Computational Methods in Subsurface Flow.* Academic, San Diego, Calif., 1985.
[13] Paniconi, C., Aldama, A. A., and Wood, E. F.: *Numerical evaluation of iterative and noniterative methods for the solution of the nonlinear Richards' equation.* Water Resour. Res., 1991, **27**:1147-1163.
[14] Wood, W. L.: Practical Time Stepping Schemes. *Oxford Univ. Press, New York, 1990*.
[15] Abriola, L.M., and Lang, J. R.: *Self-adaptive finite element solution of the one dimensional unsaturated flow equation.* Int. J. Numer. Methods Fluids, 1990, **10**:227-246.
[16] Grifoll, J., and Cohen, Y.: *A front-tracking numerical algorithm for liquid infiltration into nearly dry soils.* Water Resour. Res., 1999, **35:**2579 – 2585.
[17] Williams, G.A., and Miller, C.T.: *An evaluation of temporally adaptive transformation approaches for solving Richards' equation.* Adv. Water Resour., 1999, **22(8)**:831-840.
[18] Kavetski, D., Binning, P., and Sloan, S. W.: *Adaptive time stepping and error control in a mass conservative numerical solution of the mixed form of Richards' equation.* Adv. Water Resour., 2001, **24:**595-605.
[19] Tocci, M. D., Kelley, C. T., and Miller, C. T.: *Accurate and economical solution of the pressure-head form of Richards' equation by the method of lines.* Adv. Water Resour., 1997, **20(1):**1-14.

[20] Kavetski, D., Binning, P., and Sloan, S. W.: *Noniterative time stepping schemes with adaptive truncation error control for the solution of Richards' equation.* Water Resour. Res., 2002, **38(10)**:1211-1220.
[21] Fassino, C., and Manzini, G.: *Fast-secant algorithms for the non-linear Richards' Equation.* Commun. Numer. Methods Eng., 1998, **14**:921-930.
[22] Jones, J. E., and Woodward, C. S.: *Preconditioning Newton-Krylov methods for variably saturated flow, in XIII International Conference on Computational Methods in Water Resources*, edited by G. F. Pinder, 101–106, A. A. Balkema, Brookfield, Vt., 2000.
[23] Lehmann, F., and Ackerer, P. H.: *Comparison of iterative methods for improved solutions of the fluid flow equation in partially saturated porous media.* Transp. Porous Media, 1998, **31:**275–292.
[24] Simunek, J., Huang, K., and van Genuchten, M. T.: *The SWMS-3D code for simulating water flow and solute transport in three-dimensional variably saturated media.* Research Report No. 139, US Salinity Lab., Riverside, CA, 1995.
[25] 3D FEMFAT. See www.scisoftware.com
[26] Forsyth, P. A., Wu, Y. S. and Pruess, K.: *Robust numerical methods for saturated-unsaturated flow with dry initial conditions in heterogeneous media.* Adv. Water Resour., 1995, **18**:25-38.
[27] SVFLUX. See www.sv_ux.com
[28] Yeh, G. T.: *FEMWATER: A Finite Element Model of Water Flow through Saturated-Unsaturated Porou.* Media (ORNL-5567=RI edn). Oak Ridge National Laboratory: Oak Ridge, TN.
[29] FLUENT. http://www.fluent.com
[30] Rathfelder, K. and Abriola, L. M.: *Mass conservative numerical solutions of the head-based Richards equation*. Water Resour. Res. 1994, **30**: 2579–86.
[31] Milly, P. C. D.: *A mass-conservative procedures for time-stepping in models of unsaturated flow*. Adv. Water Resour., 1985, **8:**32-36.
[32] Pan, L., Warrick, A. W., and Wierenga, P. J.: *Finite element methods for modeling water flow in variably saturated porous media: numerical oscillation and mass-distributed schemes*. Water Resour. Res., 1996, **32**:1883-1889.
[33] Brooks, R. H. and Corey, A. T. :*Properties of porous media affecting fluid flow*. J. Irrig. Drain. Div. Am. Soc. Civ. Eng., 1966, **92:**61–88.
[34] van Genuchten, M. T.: *A Closed-form Equation for Predicting the Hydraulic Conductivity of Unsaturated Soils.* Soil Sci. Soc. Am. J. 1980, **44:**892–898.
[35] Allen, M. B., and Murphy, C. L.: *A finite element collocation method for variably saturated flow in two space dimension.* Water Resour. Res. 1986, **3(11):**1537-1542.
[36] Zadeh, K. S. and Shah, S. B.: *Mathematical modeling and parameter estimation of axonal cargo transport*. J. Comput. Neurosci., 2010, **28(3):**495–507.
[37] Zadeh, K. S.: *Parameter estimation in flow through partially saturated porous materials.* J. Comput. Phys., 2008, **227(24)**:10243–10262.
[38] Paniconi, C., and Putti, M.: *A comparison of Picard and Newton iteration in the numerical solution of multidimensional variably saturated flow problems.* Water Resour. Res., 1994, **30**:3357–3374.
[39] Cooley, R. L.: *Some new procedures for numerical solution of variably saturated flow problems.* Water Resour. Res. 1983, **19**:1271-1285.
[40] Huyakorn, P. S., Springer, E. P., Guvanasen, V., Wadsworth, T. D., 1986. *A three dimensional finite element model for simulating water flow in variably saturated porous media.* Water Resour. Res. 22, 1790-1808.
[41] Ababou, R., Gelhar, L . W. and McLaughlin, D.: *Thee-dimensional flow in random porous media.* vol. 2, Rep. 318, Ralph M. Parsons Lab., Mass. Inst. of Technol., Cambridge, 1988.
[42] Paniconi, C. and Wood, E. F.: *A detailed model for simulation of catchment scale subsurface hydrologic processes*. Water Resour. Res., 1993, **29(6):**1601-I620.
[43] Casulli, V. and Zanolli, P.: *A nested Newton-type algorithm for finite volume methods solving Richards' equation in mixed form.* SIAM J. Sci. Comput., 2010, ***32***:2255–2273.
[44] D'Haese, C. M. F., Putti, M., Paniconi, C., and Verhoest, N. E. C.: *Assessment of adaptive and heuristic time stepping for variably saturated flow.* Int. J. Numer. Methods Fluids, 2007, **53:**1173–1193.
[45] Islam, M.S., Paniconi, C. and Putti, M.: *Numerical Tests of the Lookup Table Method in Solving Richards' Equation for Infiltration and Drainage in Heterogeneous Soils.* Hydrology, 2017, **4(33)**.

[46] McBride, D., Cross, M. Croft, N., Bennett, C., and Gebhardt, J.: *Computational modeling of variably saturated flow in porous media with complex three-dimensional geometries.* Int. J. Numer. Methods Fluids, 2006, ***50***:1085–1117.
[47] Islam, M.S.: *Consequence of backward-Euler and Crank-Nicolson techniques in the finite element model for the numerical solution of variably saturated flow problems.* J. KSIAM, 2015, **19(2)**:197-215.